RSC Advances

ROYAL SOCIETY OF CHEMISTRY

PAPER

View Article Online
View Journal | View Issue

Cite this: *RSC Adv.*, 2026, **16**, 23754

Shelf life and time-resolved thermal, chemical, and thermodynamic characterization of four hydrophobic deep eutectic solvents

Adewale Ajose, * Gary A. Leeke, Pritha Sen, Preeti Singh, Pratik Kokane, Syed Altaf and Matthew J. Keith

Hydrophobic deep eutectic solvents (HDESs) are increasingly recognized as green alternatives to traditional organic solvents in extraction, catalysis, and polymer processing; however, their long-term stability remains poorly understood. This study investigated the critical gap in systematically characterizing the effects of long-term storage on four thymol-and tetraoctylammonium bromide (TOAB)-based HDESs with decanoic (C10) and dodecanoic (C12) over 20 weeks of storage. Weekly comprehensive measurements and characterization techniques were used to monitor changes in both bulk properties and molecular structures. Thermal stability was evaluated using differential scanning calorimetry (DSC) and thermogravimetric analysis (TGA), which consistently showed onset decomposition temperatures between 136 °C and 205 °C across all four solvents, with a variation of ±2.77 °C over the 20-week storage period. TOAB- based systems exhibited superior thermal stability, likely due to ionic hydrogen bond networks. Thermodynamic analysis revealed that molar excess Gibbs free energy values satisfied the non-ideality criterion $\left(\frac{gE}{RT} < -1/3\right)$, and activity coefficients remained well below unity throughout the study, confirming strong intermolecular interactions and eutectic integrity. Fourier-transform infrared (FTIR) spectra showed consistent features with no signs of chemical degradation or moisture-induced structural changes. The C12-based systems undergo reversible room temperature crystallisation attributed to segregation of a fatty-acid-rich solid phase; this microphase separation modifies processability but not the underlying eutectic chemistry. Density (0.88–0.95 g cm^{-3}), viscosity (18–85 mPa s @ 25 °C), and apparent pH remain within the acidic range expected for carboxylic acid-based HDESs, with observed fluctuations attributed mainly to the known limitations of glass electrodes in low conductivity media rather than genuine chemical change. These findings demonstrate that TOAB- and thymol-based HDESs are thermally and chemically stable during the storage period. This research contributes to an important knowledge gap in green solvent technology and supports their further development from laboratory research to industrial applications.

Received 11th February 2026
Accepted 25th April 2026

DOI: 10.1039/d6ra01239f

rsc.li/rsc-advances

1. Introduction

Deep eutectic solvents (DESs) are a class of designer liquids formed from the interaction of two or more components; specifically, a hydrogen bond donor (HBD) and a hydrogen bond acceptor (HBA), which uniquely interact through strong hydrogen bonding to generate an eutectic mixture with a melting point below that of the individual components.[1–5] They are considered green alternatives to conventional volatile organic solvents such as tetrahydrofuran (THF) and dichloromethane (DCM), because they have negligible vapour pressure, offer tunability of polarity, viscosity, and solvating power, and cost-effective production, often with bio-derived constituents.[4,6,7] Within this broad family, natural deep eutectic solvents (NADES) often comprising of natural metabolites such as those based on sugars (for example, glucose: fructose: water, and sucrose-based mixtures) or amino acids (like proline: glycerol, glycerine: glycerol systems) are generally reported to exhibit low toxicity, good biocompatibility and ease of preparation, which has led to their growing use in pharmaceutical and biomedical applications.[8–11] At the same time, many commonly studied DES are hydrophilic: they are highly polar, strong water miscible, and can display relatively high viscosities, features that are advantageous for certain separations and catalytic processes but also introduce important limitations.[2,4,12,13]

Hydrophilic DESs perform well in applications that exhibit their polarity and water miscibility, such as the extraction of polar compounds, electrochemistry, and catalysis, and they

School of Chemical Engineering, University of Birmingham, Edgbaston Park Road, Birmingham, B15 2TT, UK. E-mail: ama457@student.bham.ac.uk

retain their properties, such as non-flammability (due to very low pressure), chemical stability, biodegradability, and biocompatibility.[6,13] However, their strong affinity for water can hinder phase separation, complicate solvent recovery, and limit their importance in biphasic systems, while their high viscosity can cause mass-transfer limitations. These drawbacks encourage the development of alternative eutectic formulations that preserve the green credentials of DESs while offering lower water miscibility and more favourable characteristics for hydrophobic systems.[14,15] In addition, earlier research mainly focused on hydrophilic choline chloride-based DESs, examining water-related phenomena such as compositional drift, moisture absorption, and hydrogen-bond reorganization during accelerated aging or repeated use.[16–18] Those studies usually investigate a single property (*e.g.*, conductivity or viscosity) over short periods (days or weeks) and rarely explore hydrophobic formulations. On the other hand, the long-term stability and shelf-life of hydrophobic DESs, especially thymol- and tetraoctylammonium-based HDES, remain largely undocumented despite their increasing use in catalysis, extraction, and polymer processing.[19–21]

Hydrophobic deep eutectic solvents (HDESs) have emerged as alternatives. They are typically synthesized from at least one component with a long alkyl chain (for example, fatty acids or natural terpenes such as thymol and menthol), which imparts macroscopic hydrophobicity and low aqueous solubility to the mixture. Like other DESs, HDESs are characterised by pronounced eutectic depression of the melting point, extensive hydrogen-bonded networks, and the ability to tailor properties such as hydrophobicity, viscosity, and solubility by varying the HBA/HBD identities and molar ratios.[2,15,22] Their immiscibility with water and many aqueous phases enables phase separation and facilitates their use as extraction media, particularly for non-polar organic compounds, pigments, pesticides, volatile fatty acids, and poorly water-soluble drugs.[14,15] Based on these qualities, HDESs effectively address the key limitation attributed to hydrophilic DESs, especially their water miscibility, while maintaining the environmental benefits associated with DESs more broadly.[14,23] For example, fatty acids and natural terpenes contribute to water immiscibility by forming distinct phases in aqueous solutions.[14]

Some of the industrial applications of HDEs, as shown in Fig. 1, are: (i) applied in the polymer processing and material science for polymer degradation, modification, and to synthesize functional polymeric materials like films, composites, and gel.[3,4] (ii) extraction of organic compounds and metal ions, where they are used in liquid–liquid extraction to isolate high-value compounds like pharmaceuticals and bioactive molecules from complex mixtures, wastewater, and natural products.[14,24] (iii) used as solvents and media for organic synthesis and multi-component reactions in green synthesis and catalysis applications[25] (iv) used to extract valuable antioxidants, colours, flavours, and other components from agricultural sources in the agriculture and food industry.[24] (v) conversion processes for the production of platform chemicals like 5-hydroxymethylfurfural from biomass in biorefineries and biomass valorization.[14]

Despite the advantages, understanding the long-term stability and shelf life of HDESs remains limited. Research has mainly focused on initial physicochemical properties, often ignoring changes during extended storage.[14] However, there is a lack of published studies that investigate or examine the stability of hydrophobic DESs. Therefore, it remains uncertain whether HDESs retain their properties after preparation and prolonged storage. This uncertainty hinders the transition of these HDESs from laboratory demonstration to commercial use, where process performance is reliant on long-term stability.

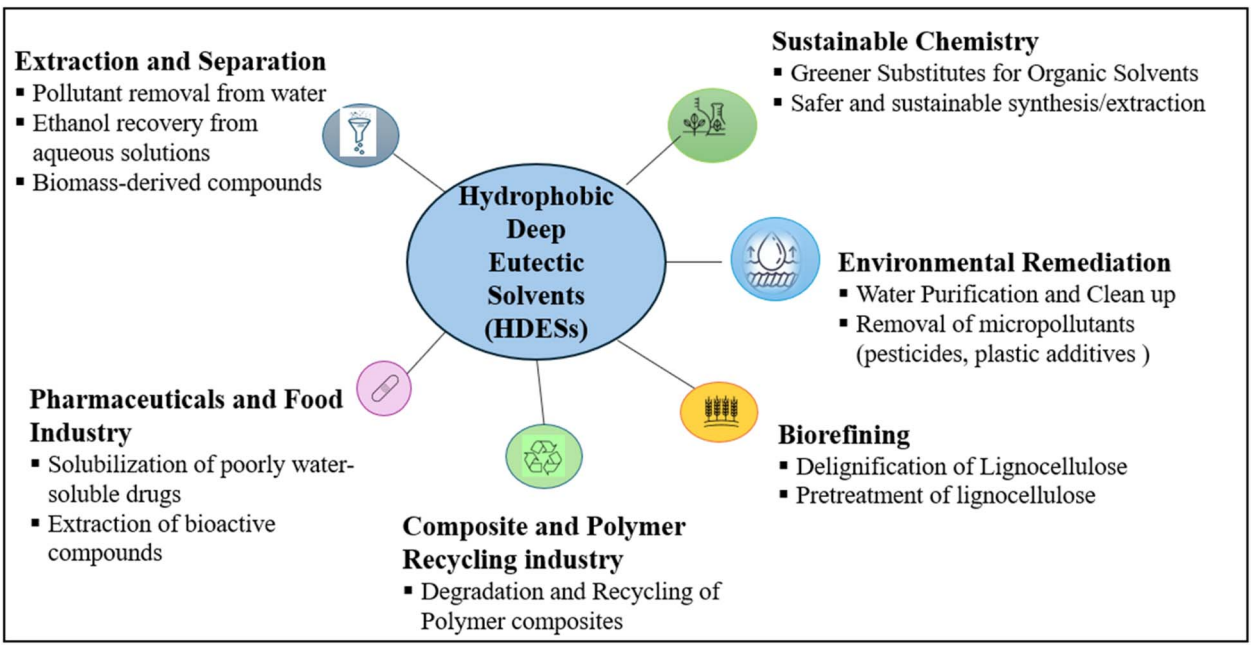

Fig. 1 Industrial application and relevance of HDESs.

Table 1 Chemical suppliers and properties[a]

Chemical reagent	Role in DES formation	Class	Supplier	Purity
(TOAB) $[CH_3(CH_2)_7]_4NBr$	Hydrogen bond acceptor (HBA)	Ionic hydrophobic (quaternary ammonium salts) with long alkyl chains	VWR internationals	>98%
Thymol $C_{10}H_{14}O$	Hydrogen bond acceptor (HBA)	Terpenes	Sigma Aldrich	>98%
Dodecanoic acid $C_{12}H_{24}O_2$	Hydrogen bond donor (HBD)	C12-carboxylic acid & a saturated fatty acid	Thermo Scientific chemicals	98%
Decanoic acid $C_{10}H_{20}O_2$	Hydrogen bond donor (HBD)	C10-carboxylic acid & a saturated fatty acid	Fisher Scientific limited	99%

[a] Nitrogen gas (N5.5) with 99.9995% purity, which is used for the thermal analyses and density measurement, was supplied by BOC.

The present work fills the gap by providing a 20-week, time-resolved multi technique assessment of four industrially relevant (Fig. 1) HDESs (thy: C10, thy: C12, TOAB: C10, TOAB: C12), combining viscosity, apparent pH, density, FT-IR, DSC, TGA and derived thermodynamic parameters (activity coefficients and excess molar Gibbs free energy). This combination of hydrophobic formulations, durations, and thermodynamic analyses enables the process to quantitatively identify which solvent properties are robust to storage and which are sensitive to structural reorganisation or partial crystallisation.

This study focused on the evolution of (i) bulk properties that govern handling and transport (density, viscosity), (ii) operational stability metrics (onset decomposition temperature, DSC transition temperatures), (iii) molecular structure (FT-IR), and (iv) thermodynamic descriptors of non-ideality and eutectic integrity (activity coefficients γ_i and reduced excess Gibbs free energy $\frac{gE}{RT}$). Mechanistically, any storage-induced changes in these variables would indicate, respectively, changes in packing efficiency or micro-void formation, reorganisation of hydrogen-bond/ionic networks, moisture uptake, or partial demixing of HBA and HBD.[26,27]

2 Materials & methods

2.1 Materials

The chemicals used in this study are listed in Table 1. All were of analytical grade and were used as received without further purification and were stored in sealed containers at room temperature, away from light and humidity.

2.2 Preparation of HDESs

The HDESs were synthesized by direct heating and stirring. The specific molar ratios correspond to their eutectic point, the combinations of which are shown in Fig. 2. Thymol : decanoic acid (C10) and thymol : dodecanoic acid (C12) were weighed in the molar ratio 1 : 1 to enable stable and homogeneous liquid formation, as in other experimental studies.[28,29] TOAB: C10 and TOAB: C12 were mixed in a 1 : 2 molar ratio. The weighed components were transferred to a beaker with a magnetic stirrer bar, and the mixture was heated to 60 ± 2 °C using a hot plate. Continuous stirring was maintained at 200 rpm until a homogenous solution was formed. The HDES was allowed to cool to room temperature between 18–24 °C and stored in

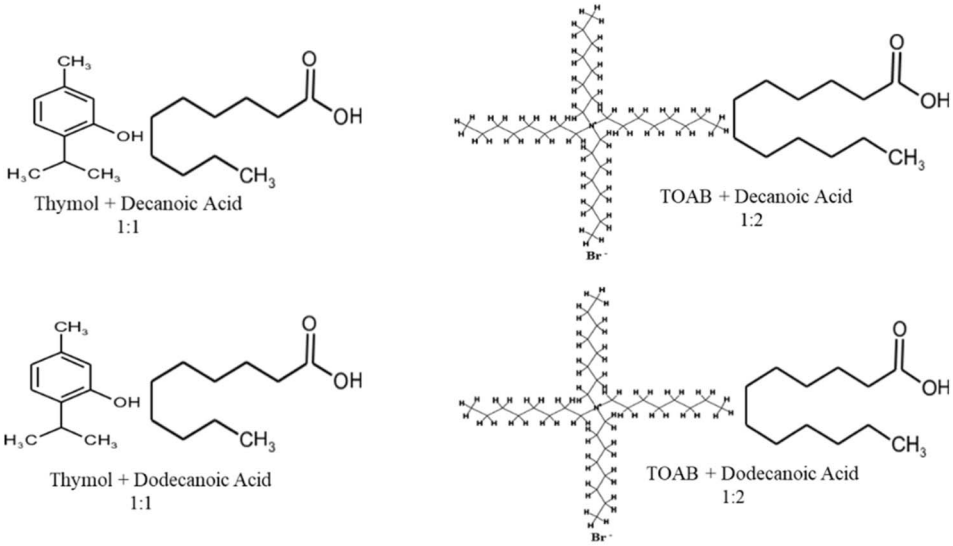

Fig. 2 Structural and stoichiometric analysis of the HDESs investigated.

airtight containers (Duran bottles) in a dark cabinet to prevent absorption of (-moisture and air), photodegradation, and any possible contamination of the samples, which may alter their composition and properties.

Quality control measures such as visual inspection and preliminary viscosity measurements were conducted post-synthesis to ensure the consistency and successful formation of each DES batch.

2.3 Characterization techniques

The characterized HDESs were analyzed using various techniques to investigate their long-term stability over 20 weeks; measurements were taken at weekly intervals throughout the study from weeks 1 to 12, with a final measurement taken at Week 20. Each of the techniques used was to assess different key properties relevant to HDES applications. Rheology measurements were taken to assess possible viscosity changes affecting handling, transport, and mixing. FTIR was used to detect any chemical changes, decomposition, or new impurities by monitoring molecular bonds. Thermal properties were monitored through TGA (for measuring thermal stability) and DSC to examine the phase transitions and crystallinity changes, while thermodynamic properties were measured from the melt temperature estimated from the DSC thermograms. Density was also monitored as detailed in the following sections. The six characterization techniques used in this work provided a comprehensive evaluation of both chemical and physical stability over time, important for shelf-life investigation. In addition, due to the semi-crystalline formation of thymol and TOAB: C12 HDESs after 24 h of synthesis (see Fig. 3), the sample bottles need to be slightly heated (≤30 °C) until a liquid formation is achieved before the samples were taken for characterisation.

Unless otherwise stated, density measurements were performed in triplicate and reported as mean ± standard deviation; viscosity measurements were repeated once per week for each HDES and compared against instrument precision limits. DSC and TGA measurements were performed weekly from week 1 to 12 and again at week 20. FT-IR and apparent pH measurements were repeated at least twice at each time point to check for instrumental drift. For clarity, only data from weeks 0, 4, 8, 12, and 20 are shown in the figures; however, the full weekly dataset (Fig. S1–S3 and Table S4) confirmed the reproducibility of the thermal transitions over the entire storage period.

2.3.1 Physical properties

2.3.1.1 Viscosity measurements. Viscosity measurements were performed using a Malvern Kinexus viscometer equipped with a Peltier parallel plate system, featuring the PU20/PL65 geometry. Measurements were made across a temperature range of 20–120 °C, maintaining a steady shear rate of 10 s^{-1} and a ramp rate of 5 °C min^{-1} with a 1 mm gap setting. The instrument precision limits for the Kinexus rheometer are between 1–2%. For this work, a single measurement was taken for each solvent per week.

2.3.1.2 Density measurements. The volumetric properties of the solvents, which indicate changes in composition or purity,

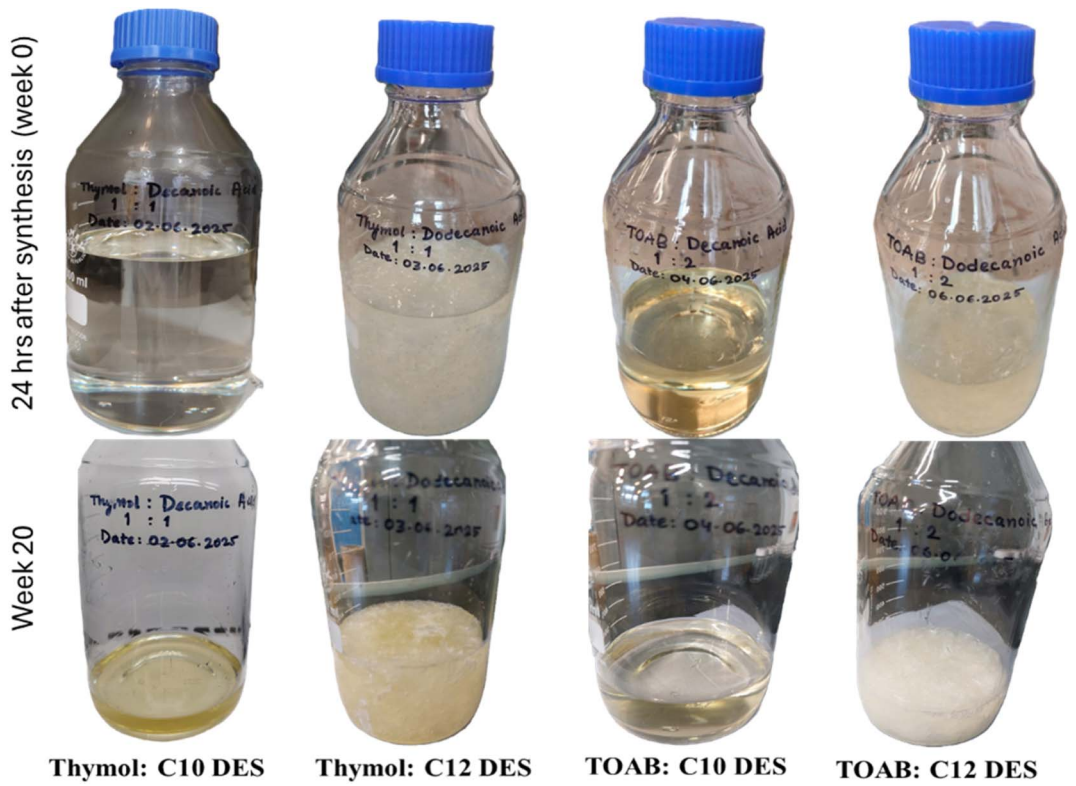

Fig. 3 Physical state of the four HDESs after synthesis and storage.

were measured using an Anton Paar Ultrapyc 5000 Pycnometer with a precision limit for repeatability between 0.05–0.15%. All measurements were performed at a temperature of 25 °C using the Nano cell (0.25 cm^3). All the densities were determined as weekly triplicate averages.

2.3.2 Chemical properties

2.3.2.1 Fourier-transform infrared (FT-IR) analysis. Fourier Transform Infrared Spectroscopy was conducted using a Thermo Fisher Scientific Nicolet 102A Summit X FTIR spectrometer. Spectra were collected over a scan range of 400–4000 cm^{-1} with a resolution of 4 cm^{-1} and 16 scans per spectrum. Samples were prepared by placing a small droplet of the DES on the attenuated total reflectance (ATR) crystal plate, and measurements were taken at regular intervals to monitor any shifts or changes in peaks, which would indicate chemical degradation or structural alterations. The spectra were processed and analyzed using Spectra analysis software, "Spectragryph". The peaks and bands were also identified within the software using the InstaNano FT-IR spectra identification table.[30]

2.3.2.2 pH measurements. The pH of the four solvents was measured using a Thermo Scientific Orion Star A211 pH meter equipped with a Hach's glass pH electrode. The meter was calibrated daily with standard buffer solutions of 4.00, 7.00, and 10.00 at a controlled temperature of 25 °C. Approximately 5 mL of each HDES's sample was used for the measurement.

2.3.3 Thermal properties

2.3.3.1 Thermogravimetric analysis (TGA). The thermal stability profiles, including decomposition temperatures and mass loss, were measured using a SCIMED EXTAR 6000-1/G/DTA 6300 thermogravimetric analyzer. Approximately 15–22 mg of each solvent sample was heated from room temperature to 600 °C at a consistent rate of 10 °C min^{-1} under an inert nitrogen atmosphere with a flow rate of 20 mL min^{-1}.

2.3.3.2 Differential scanning calorimetry (DSC) analysis. Differential scanning calorimetry was performed using a Hitachi DSC 101 to study the thermodynamic transitions in the HDES. Approximately 10–15 mg of each DES sample was weighed into an aluminium sealed pan. The samples were subjected to heating and cooling cycles within a temperature range of −80 to 350 °C at a rate of 10 °C min^{-1}. Thermal transitions such as melting points, crystallization temperatures, and glass transition temperatures were monitored over the period under investigation to identify phase transformations.

2.3.3.3 Thermodynamic characterisation. The thermodynamics of the HDES were characterized using the melt temperature data from the DSC thermograms. These data were used to evaluate the activity coefficients, molar Gibbs' free energy, and how these important thermodynamic properties changed over time (within storage period).

3 Results and discussion

3.1 Physical properties

3.1.1 Physical state. Alongside quantitative measurements, the visual state of each of the four HDESs 24 h after preparation and after 20 weeks of storage is shown in Fig. 3. The C10-based HDESs (thymol: decanoic and TOAB: decanoic acids) remain as clear homogeneous liquids with no sign of any crystallisation.

The visual inspection reveals no macroscopic biphasic liquid–liquid separation; instead, the systems evolve into a semi-crystalline solid with embedded liquid domains and melted completely after mild heating (≤30 °C). Thus, crystallisation primarily impacts processability (*e.g.*, handling and pumping) rather than altering the underlying eutectic chemistry, provided that operating temperature remains above the melting point, as this can decrease liquid-phase stability due to the increased van der Waals interactions that promote crystallization.[31,32]

Additionally, the spontaneous solidification of C12-HDES systems implies that at room temperature, the stored systems cross from a fully eutectic into a regime where part of the mixture lies outside the single-phase liquid domain. The overall composition remains the original eutectic ratio, but crystallisation of a C12-rich phase likely occurs, enriching the residual liquid in the complementary component and altering the effective HBA: HBD ratio. This scenario is consistent with the observed higher viscosity and density sensitivity of the C12 systems, which would be expected if the remaining liquid is slightly off eutectic.

The absence of new FT-IR bands and the reproducibility of DSC transition temperatures over 20 weeks (section 3.2.2 and 3.3.3) show that crystallisation is not accompanied by detectable chemical degradation or formation of new phases at the molecular level. The C12 behaviour was therefore interpreted as reversible solid–liquid microphase separation driven by enhanced dispersion interactions between the longer alkyl chains, rather than loss of eutectic integrity.

In relation to industrial applications, the room temperature crystallisation of the C12 systems implies that, in continuous processes, these formulations may require mild heating of storage tanks and transfer lines (25–30 °C) to avoid solidification and ensure reliable pumping and mixing. In contrast, the C10 HDES remain fully liquid at ambient conditions and therefore appear better suited to large-scale handling, on-demand make-up, and closed-loop recycling without additional thermal management.

3.1.2 Density measurement. Density measurement is one of the key fundamental properties of a solvent that indicates molecular packing and interaction. It provides insight into the phase stability, purity, and compositional changes of the hydrophobic solvents over time; therefore, it is a very important parameter in measuring the long-term stability of the solvents, especially for industrial applications, as described by Chen *et al.*[33]

The four HDESs show good stability and molecular structure preservation with a small increase over the 20 weeks. The data points have relatively small error bars with similar week-to-week variations across the bars for the three repeats (Fig. 4), indicating good reproducibility. This provides confidence in a consistent profile and stability of the density measurement for the four HDESs over the study period.

The density measurements range between 0.9713–0.9897 g cm^{-3} for thymol: C10; 0.9209–0.9543 g cm^{-3} for thymol: C12; 0.965–0.9898 g cm^{-3} for TOAB: C10; and 0.9203–

0.9544 g cm^{-3} for TOAB: C12. The mean density and variability of the four HDESs over the 20 weeks are summarised in Table 2.

As presented in Table 2, the overall average density was calculated for each HDES, and the variability over the 20-week storage period was expressed as relative standard deviation (RSD %). The nano cell used for the density measurements has an accuracy of ±1.00% and repeatability of ±0.50%.[34] The calculated RSDs ranged from 0.40 to 0.65% across the four HDESs, and these values fall within the stated performance limits of the nano-cell configuration of the Antonn Paar Ultrapyc 5000, indicating that no meaningful drift occurred during storage. The small density variation may have arisen from experimental uncertainty rather than density drift, confirming the long-term physical stability of the HDES. The average density results aligned with the literature values for similar hydrophobic deep eutectic systems as published by Zainal-Abidin *et al.*[15] and Duque *et al.*[35]

However, the slightly higher variability observed for the thymol: C12 HDES system may be due to its semi-solid crystalline formation (Fig. 3), higher viscosity, and increased sensitivity to sample loading and temperature equilibration in the nano cell.

$$\text{RSD} = \frac{\text{SD}}{\text{Mean density}} \times 100 \quad (1)$$

C10 HDESs' measurements show higher sensitivity to changes in density with time and conditions than the longer alkyl chain dodecanoic acid measurements, with a decrease in density values as the fatty acid chain lengthens due to the increased free volume and reduced molecular packing efficiency.[35] However, in comparison with other DESs, choline chloride-based DESs have higher densities (1.05–1.45 g cm^{-3}) as a result of the chlorine cation. The stability observed in the measurements over 20 weeks indicates a consistent density of each solvent system, which in turn provides confidence that the volumetric requirements of an industrial process will not change following long-term storage of these HDES systems.

Table 2 Percentage variability (RSD %) of the four HDESs[a]

HDES	Mean density (g cm^{-3})	Standard deviation (SD)	RSD (%)
Thymol: C10	0.9813	0.0043	0.44
Thymol: C12	0.9380	0.0061	0.65
TOAB: C10	0.9801	0.0039	0.40
TOAB: C12	0.9387	0.0049	0.52

[a] The relative standard deviation (RSD, %) was calculated using eqn (1).

3.1.3 Rheology investigation. Viscosity is considered one of the most important physical properties of deep eutectic solvents, as it affects their pumping requirements, mixing efficiency, mass transfer, extraction performance, and solvent–

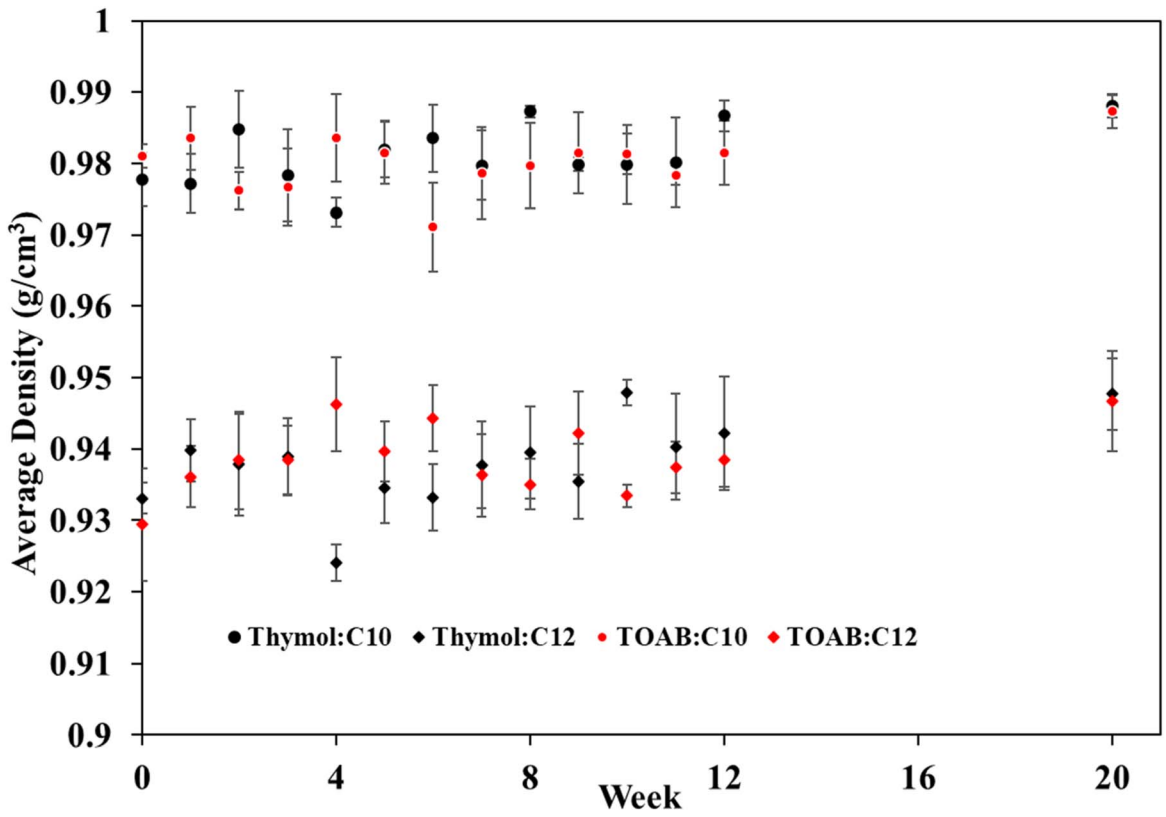

Fig. 4 Average densities of each of the four HDESs were measured for weeks 1 to 20. (Error bars show the spread of triplicate measurements and are reported as mean ± standard deviation).

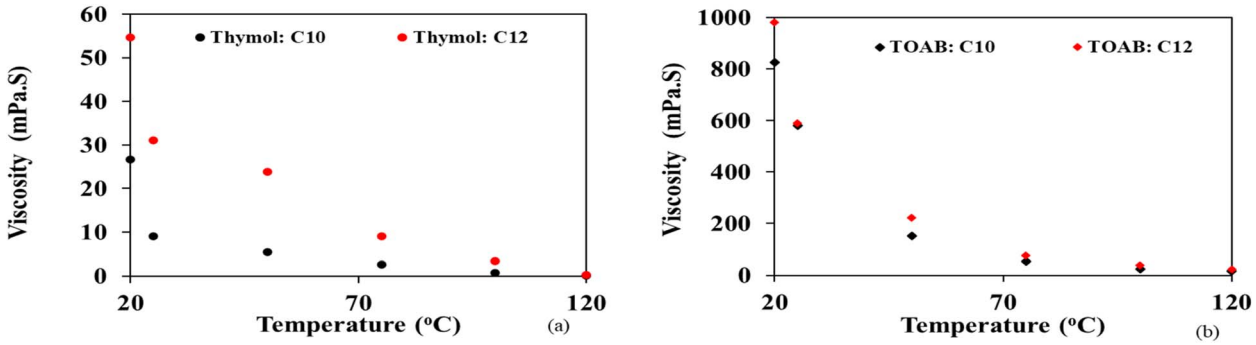

Fig. 5 Viscosity-temperature curves for (a) thymol-based HDESs, and (b) TOAB-based HDESs for the 20- week measurements.

solute interactions.[5] Additionally, Pietro *et al.*[36] and Gygli *et al.*[37] proposed that viscosity is widely regarded as a key indicator of DES stability; therefore, it should be monitored regularly to evaluate the impact factors such as aging, water content, or thermal stress on DES properties. Example rheology curves for each solvent are shown across the temperature range investigated in Fig. 5. The viscosity values for the four HDES decreased consistently with increasing temperature, which aligns with the fundamental property of fluids. This is due to higher temperatures providing more kinetic energy to the molecules, allowing them to overcome intermolecular forces, enabling them to flow more easily.[37,38]

All the experimental viscosity values/ranges presented in Fig. 5 align with the literature values for both thymol and TOAB-based HDES. Both curves' patterns suggest that the solvents are resistant to chemical degradation and compositional changes.[14,39–41] It was also observed that thymol-based HDESs are consistently less viscous than TOAB-based HDESs, and that the longer the fatty acid chain, the more viscous the solvent becomes.

As observed in Fig. 6, the four HDES combine high stability and low viscosity over a long-term storage period. The week-to-week consistency and reproducibility are indications of their excellent long-term stability, intact flow properties due to the strong intermolecular interactions, which maximize solvent reuse and reduce resource input and chemical waste. The percentage variations for each solvent across the temperatures vary by ±10% across the 20 weeks; however, the manufacturer's documentation for the Kinexus rheometers only specifies torque, gap, and temperature resolutions, but does not give a single "instrument relative error" for viscosity.[42]

As suspected based on the observations illustrated in Fig. 3, the crystalline phase formation of both C12 HDES results in higher viscosity data in comparison to the C10 HDES. Higher crystallinity can increase viscosity as the structures inhibit molecular mobility and flow, raising the energy barrier for bulk

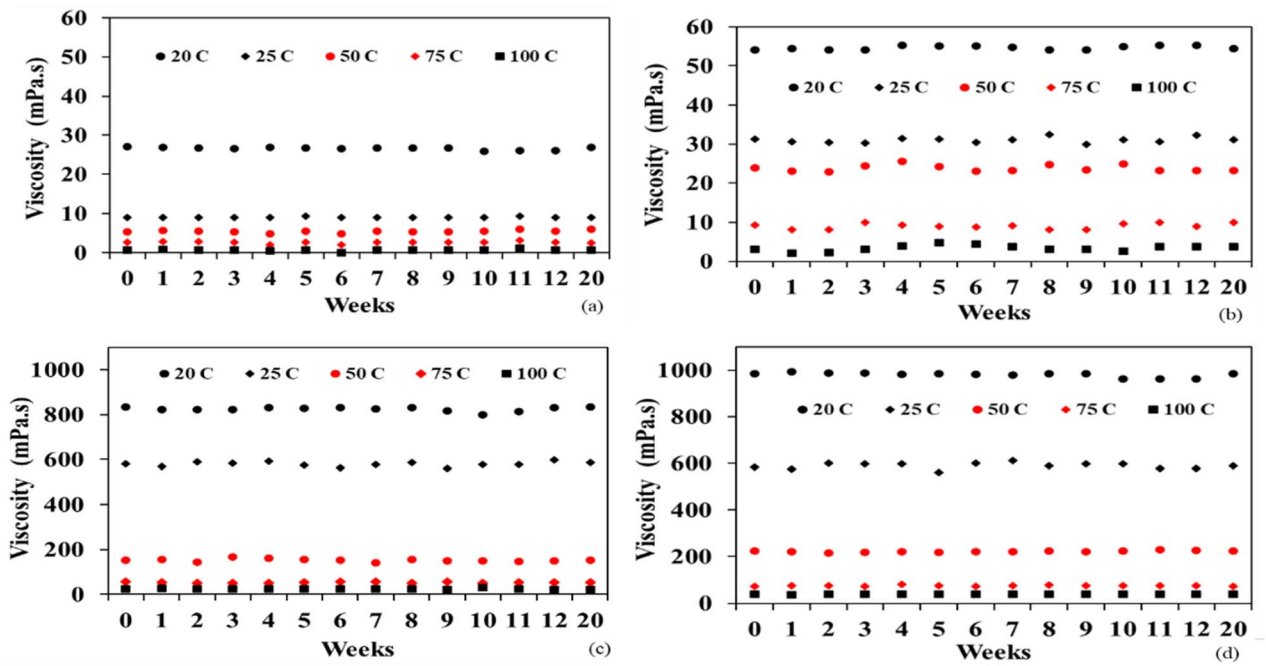

Fig. 6 Multi-week experimental viscosity graphical representation at different temperatures, (a) thymol: C10; (b) thymol: C12; (c) TOAB: C10; and (d) TOAB: C12.

fluid movement. Complete melting, and subsequently higher temperatures, yield lower viscosity, which will reduce the pumping and/or mixing energy requirement. An important design consideration is the compromise between the energy input to raise the temperature and the energy saving due to the reduction in the mechanical power requirements.

Our observation that viscosity serves as a sensitive probe of DES microstructure is consistent with recent molecular simulation and experimental work, which shows that subtle rearrangements of the hydrogen-bond network and nanostructuring strongly control the temperature-dependent viscosity of DES and related eutectic liquids.[43] The limited week-to-week variation observed in this study, therefore, provides additional indirect evidence that no significant rearrangement or degradation of the HDES microstructure occurs over a 20-week storage period.

3.2 Chemical properties

3.2.1 pH measurement. While a conventional pH meter is calibrated against aqueous solutions, it can signal changes in the proton activity of the solvent. However, as stated by Doneux *et al.*[44] it is more accurate to refer to these measurements as the "apparent pH" because of the non-aqueous nature and complexity in calibrating the pH of deep eutectic solvents due to the variable compositions. The HDES studied here are essentially anhydrous and have low ionic conductivity; therefore, the quantity reported as pH does not correspond to the thermodynamic definition used for aqueous solutions. Instead, the glass electrode responds to an ill-defined mixture of proton activity, junction potential, and interfacial equilibria at the membrane solvent interface, so the measured value is best regarded as an operational indicator of acidity/basicity under a fixed calibration protocol rather than an absolute pH.[45–48] Apparent pH was only used to track possible large-scale changes in acidity during storage and rely on FT-IR and thermodynamic data to assess chemical stability.

The alkalinity and acidity of DESs can influence their chemical stability, as they can sometimes generate impurities during preparation, especially using organic acids such as decanoic and dodecanoic acid. For example, Ruggeri *et al.*[49] reported that Tetrabutylammonium chloride: Decanoic Acid (TBACl/DA) HDES formed a gel in contact with a strongly acidic aqueous environment, which generated a loss in their stability and led to a phase change. This indicates that HDESs are not universally stable across all pH ranges, especially when they are exposed to strong aqueous acidic environments.[49]

As observed in Fig. 7, the thymol-based systems (C10 and C12) start near pH around 2.1–2.4 and increase slightly to around 2.5–2.9; thereafter, the pH fluctuates at week 6–10 but remains below 3.0, indicating only minor acid-base change over the storage period. The TOAB-based systems show less acidic pH values than the thymol systems, rising from about 3.3–3.5 initially to about 4.0–4.8 by week 8–12, after which the values stabilize, suggesting a gradual shift toward less acidity before stabilization. Although there are no widely reported standard pH values for the neat thymol- and TOAB-based HDESs or similar low-polarity DESs, as pH is only considered "a property of convenience rather than a fundamental thermodynamic quantity".[50] However, Damilano *et al.* confirmed that DESs containing carboxylic acids as hydrogen bond donors are mostly acidic, with a reported range of 3 and below for thymol-based systems,[51] and a pH range of 4–8 for TOAB-based systems,[52,53] depending on temperature, molar ratio, and water content. The TOAB-based solvents show greater variability in the measurements, which is common for HDESs based on tetraoctylammonium bromide and other quaternary ammonium salts due to ionic exchange and partial leaching of the ammonium salt constituents. Within the experimental precision, the week-to-week pH trends do not correlate with changes in density, viscosity, FT-IR spectra, or thermal transition temperatures. In particular, the TOAB-based HDESs show the largest apparent pH drift but maintain constant TGA onset temperature, DSC melting transitions, and unaltered IR band

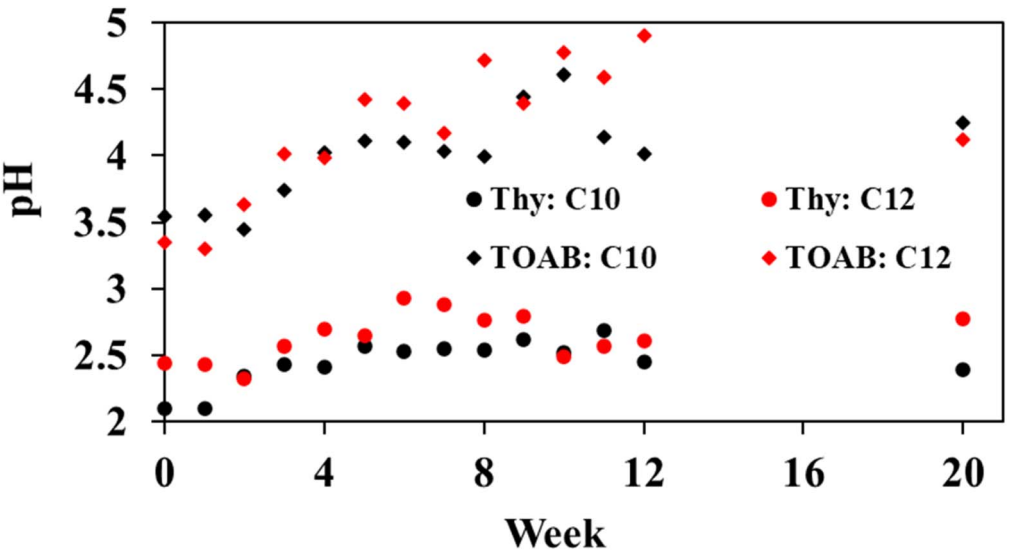

Fig. 7 Apparent pH evolution of thymol-based and TOAB-based HDESs formulated with C10 and C12 components during 20 weeks of storage.

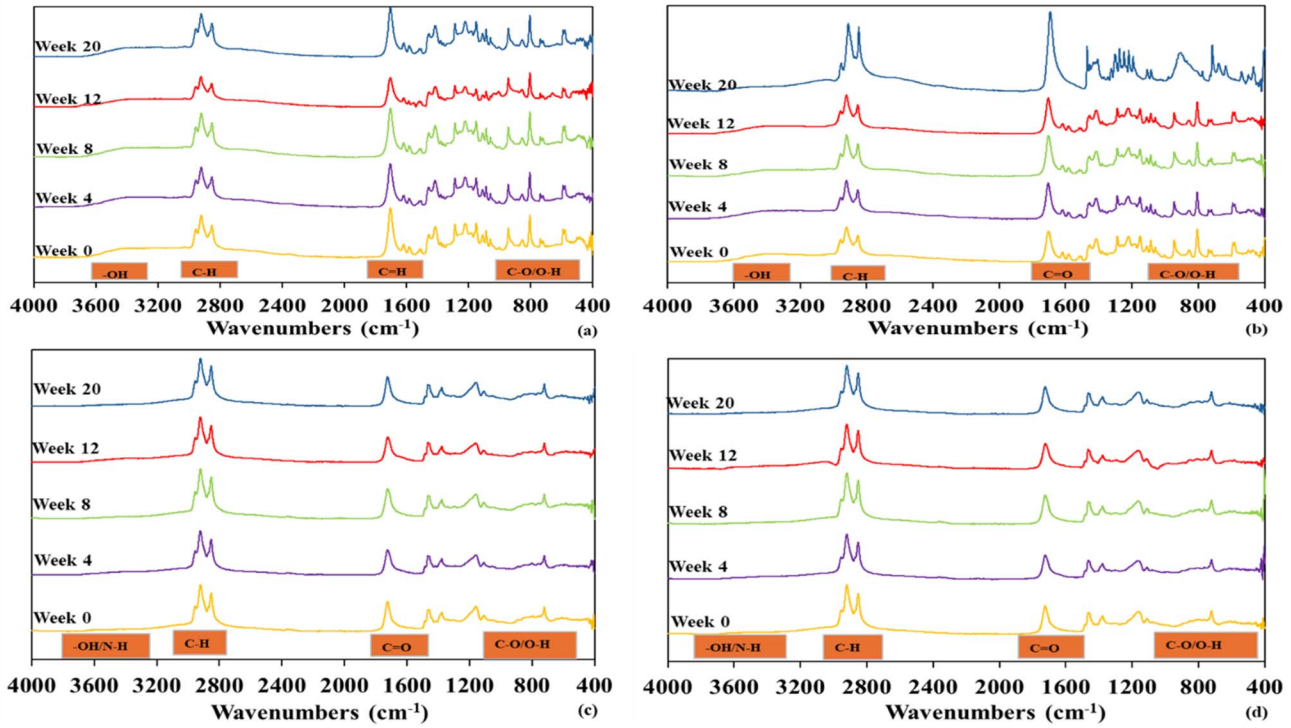

Fig. 8 FT-IR spectra for four HDESs: (a) thy: C10 DES; (b) thy: C12; (c) TOAB: C10, and (d) TOAB: C12 HDESs.

positions, which argues against substantial chemical transformation during storage.

It should also be noted that low conductivity and electrode response are observed due to the low conductivity of non-aqueous HDESs and electrode dehydration, leading to slow response times, unstable readings, and greater sensitivity to environmental changes. Exposure to air and temperature fluctuations can further destabilize the pH of HDES.

Given the low conductivity of these hydrophobic media, the use of an aqueous reference solution, and the known susceptibility of glass electrodes in non-aqueous systems to junction potential instability, partial dehydration, and slow equilibration, part of the observed pH variability, especially for TOAB-based HDES, likely reflects instrumental artefacts rather than genuine changes in proton activity. Furthermore, liquid junction potential or mismatches between sample and reference solution can be amplified in hydrophobic, low-water-content HDES, which may also be responsible for additional pH variability.[54,55] Therefore, apparent pH was treated as a qualitative indicator only and rely primarily on FT-IR and thermodynamic analysis to assess chemical stability.

3.2.2 FT-IR analysis. The infrared spectra of the four HDESs were determined to gain insights into their chemical structure and intermolecular interactions, especially hydrogen bonding between the components of thymol and TOAB-based HDES (Fig. 8) and S1 (i)–(iv). The stability and performance of these HDESs depend on the integrity of the hydrogen-bond network.[35] The main functional groups identified for thymol: C10 and thymol: C12 include O–H (hydroxyl) at 3300–3200 cm^{-1}, aliphatic C–H stretching at 2955–2850 cm^{-1}, C=O (carbonyl) at 1710–1715 cm^{-1}, CH_2/CH_3 bending at 1450–1375 cm^{-1}, and C–O stretching at 1260–1050 cm^{-1}. Meanwhile, TOAB: C10 and TOAB: C12 exhibited similar wavenumbers.[56,57] The wavenumber at 3300–3200 cm^{-1} likely corresponds to O–H/N–H (hydroxyl/amine) stretching, indicating a weaker bond compared to the thymol-based DES, due to the absence of hydroxyl groups in the TOAB system.[35,56,57] Additionally, hydrogen bonding primarily relies on ionic bonds or carboxylic acid donors.

The spectra were recorded over 12 weeks, with follow-up measurements at week 20. The slight shifts to lower wavenumbers in the C–O bands suggest an increased electron density of the carbonyl oxygen due to hydrogen bond formation between components. Despite these slight shifts and broadening observed in the spectra, there appears to be consistency with the characteristic wavenumbers and peaks of the individual precursor components, implying that there is little change in the chemical composition over the test period. Hydrogen bonding interactions between the thymol and carboxylic acid components are therefore likely well maintained over the period. Additionally, no new bands were observed at week 20, indicating the persistence of the thymol-carboxylic acid hydrogen-bonded network and the absence of degradation products, such as esters or carboxylates. There was no increased broadening of the O–H band, which would indicate moisture absorption or oxidation. This absence of change is important for the HDESs to retain their macroscopic properties and efficacy as green solvents.[35]

Similarly, TOAB: C10 and C12 systems show the same O–H and N–H stretching vibrations for the same wavenumbers that

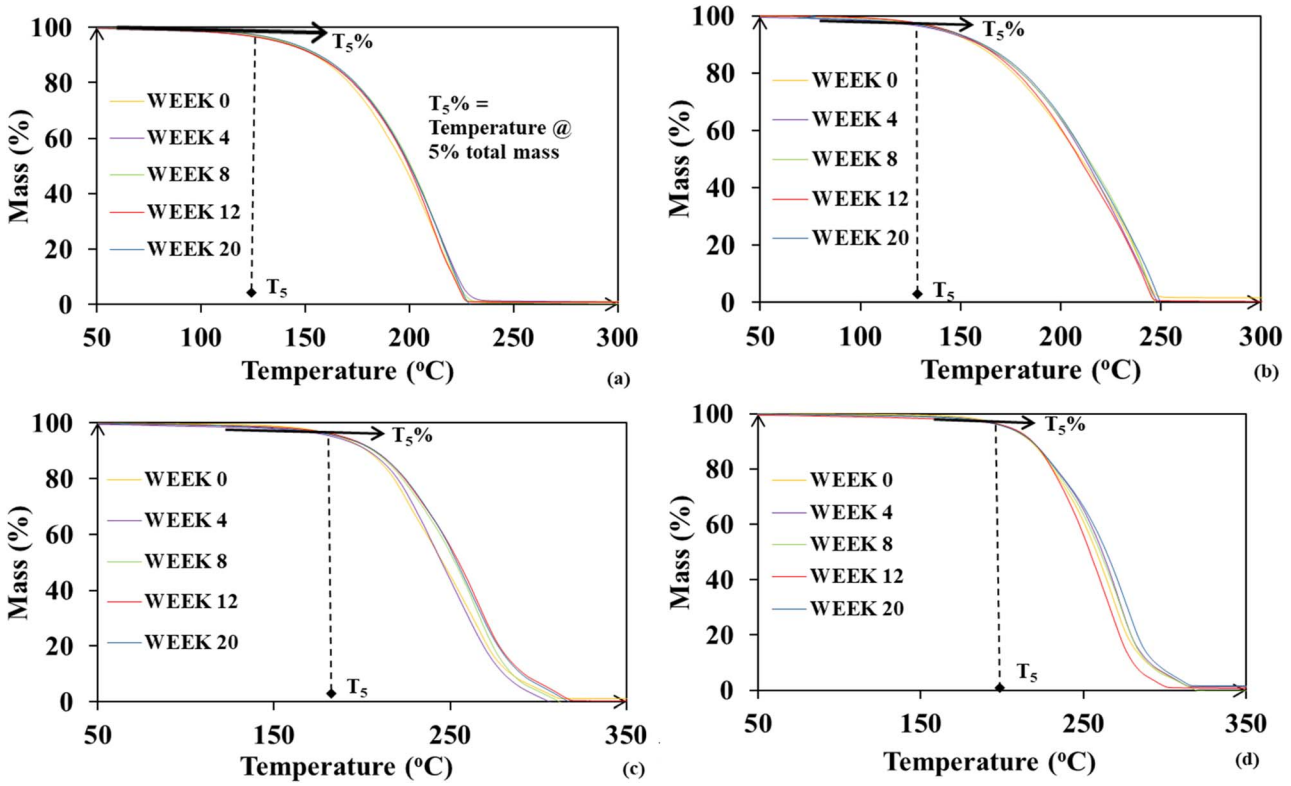

Fig. 9 TGA curves of the four HDESs: (a)thy: C10; (b)thy: C12; (c)TOAB: C10, and (d)TOAB: C12.

indicate hydrogen bond formation over the test period.[35] In addition, the characteristic absorption bands of the quaternary ammonium salts were observed in the solvent spectra. The presence of a strong band at C═O (1750–1735 cm^{-1}) indicates the formation of intermolecular hydrogen bonds.[57,58]

The uniformity and consistency of the solvent spectra in the four HDESs indicate exceptional chemical stability and extended shelf life, demonstrating that HDESs maintain their molecular structure more effectively than hydrophilic DESs by resisting moisture-induced degradation.[14,22] This also suggests that the hydrogen bonding that defines these solvents is maintained throughout the storage period.

3.3 Thermal properties

3.3.1 Thermogravimetric analysis. The TGA analysis of the four HDESs over 12 weeks, plus the additional test at week 20, is presented in, Fig. 9, (i) and (iv). The four solvents showed minimal changes or minor deflections for each solvent, implying that the instantaneous thermal profiles (onset and decomposition ranges) from the previously published work (using single dynamic TGA runs),[33,35,59,60] are similar to what was observed at each point for this work. Fig. 10 shows the variation of peak degradation temperature over storage time for the four HDESs. All the systems exhibit minimal variation (<3 °C) over 20 weeks, indicating good thermal stability during storage.

The T_5% (5% of total mass loss) was used to estimate the onset temperature of the thermal degradation for the four HDESs. It is equivalent to the temperature at which HDES begins to degrade or the first deflection from the baseline as described by ISO 11358–1 and ASTM E2550.[61,62] Furthermore, T_5% is a vital parameter in determining the operational temperature limits and long-term stability of the solvent.[63]

The onset temperature at T_5% was estimated from the TGA curve as shown in Fig. 9. The summary of the results is presented in Table 3.

The onset temperatures varied by ± 5 °C per solvent throughout the weeks, including week 20, indicating good stability. The consistent onset temperature values (*i.e.*, point where the TGA first shows a measurable deviation rather than

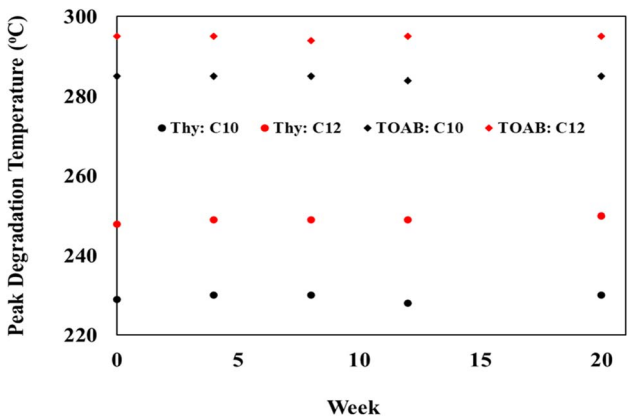

Fig. 10 Thermal stability trends across the four HDES using the peak degradation temperature (T_5%) change with storage period.

Table 3 Onset temperatures for the four HDESs as calculated from the T_5%

	Onset temperature (°C) T_5% = 5% total mass loss			
Week	Thy: C10	Thy: C12	TOAB: C10	TOAB: C12
0	139.18	140.86	187.41	203.80
4	136.93	139.46	184.21	203.88
8	138.31	143.57	189.23	203.37
12	136.48	142.20	189.74	204.85
20	140.62	143.31	187.89	203.39

substantial degradation) indicate that the solvents can effectively resist any initial thermal decomposition over a long storage period.[64,65] More importantly, the TOAB-based DESs show higher thermal stability than the thymol-based DESs, especially TOAB: C12, which shows a higher temperature threshold before any significant mass loss. According to Chen *et al.*[63] this may be due to the nature of the HBD components (tetraoctylammonium bromide), which can form a thermally resistant hydrogen bond network with the carboxylic acids when compared to thymol. This results in the observed higher decomposition onset temperature. Additionally, the higher onset temperature was observed for C12 than for C10 -based HDESs, which may be due to stronger ionic interactions, the component's lower volatility, and the influence of the HBD chain length on the thermal stability of the solvents.[33]

The small variation in T_5 ($\leq$5 °C) over 20 weeks is comparable to or smaller than differences attributed to heating-rate changes in high-resolution TGA studies,[66] reinforcing that the observed data is within experimental uncertainty rather than evidence of progressive degradation.

All TGA experiments were performed at a steady heating rate of 10 °C min^{-1}, balancing between experimental throughput and thermal lag. The absolute onset temperatures under dynamic heating are known to depend on the heating rate; higher rates typically cause degradation onsets to appear at higher temperatures due to kinetic constraints.[66,67] However, since all measurements in this study follow the same heating protocol, focussing on relative changes over time rather than absolute kinetic parameters, the systematic effect of heating rate does not impact the conclusion that HDES decomposition profiles remain consistent during storage.

3.3.2 Differential scanning calorimetry. The thermal transitions of the four solvents were evaluated by monitoring the DSC onset and peak temperatures of the primary endothermic transition, which was determined from the DSC heat flow curve using the tangent intersection method. The DSC onset temperature is sensitive to heat-capacity changes and was determined from the point where the heat-flow curve first deviates from the baseline at the start of the thermal event, such as the glass transition, melting, and/or crystallization. The peak temperature corresponds to the maximum rate of the melting process (*i.e.*, the point where the endothermic heat-flow signal is highest) and therefore occurs after the onset temperature. As observed in Fig. 11, the DSC thermograms of the four solvents under study showed reproducible transition temperatures across the 20-week storage (Fig. S3), with minor scatter in both the peak and onset temperatures.

The primary DSC endotherm for thymol: C10 DES shows onset temperatures near 92 °C and peak temperature around 98 °C, while those of thymol: C12 DES are around 93 °C and 96 °C. In comparison, the TOAB-based DES showed higher onset and peak temperatures, consistent with stronger ionic interactions with TOAB: C10 DES measured about 189 °C and 229 °C, respectively, and TOAB: C12 DES around 209 °C and 245 °C, respectively. Overall, the consistent onset and peak temperature data over time provide strong evidence that all four HDESs

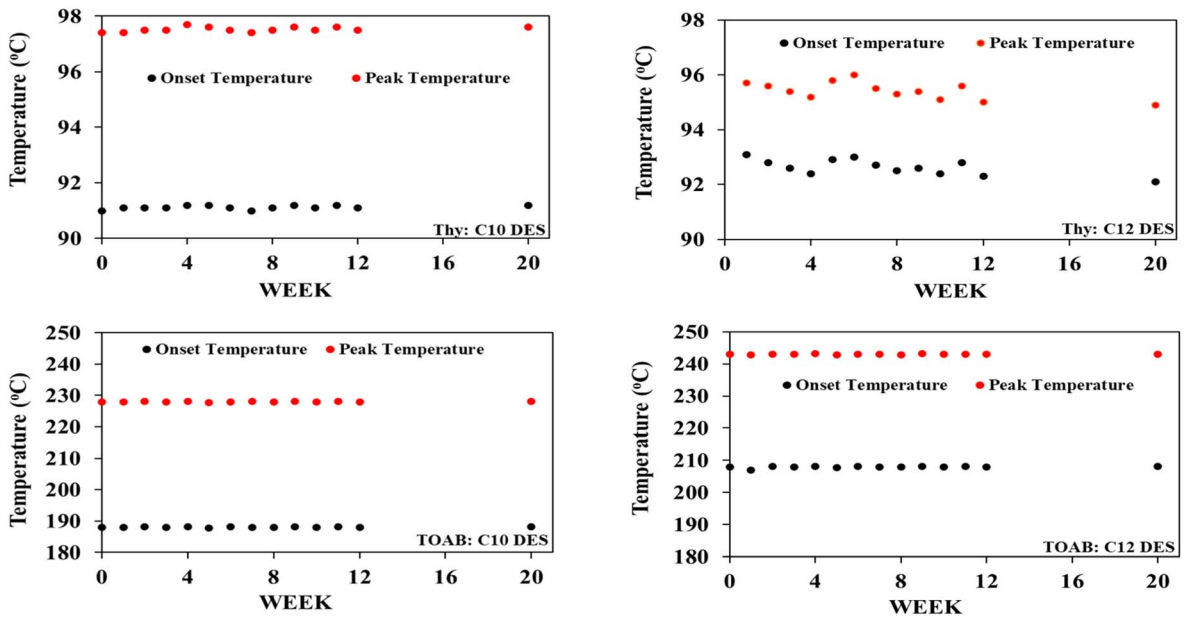

Fig. 11 Endothermic-DSC onset and peak temperature for the four HDES over the storage period.

remain thermally stable during the storage period under the tested conditions.

3.4 Thermodynamics of HDES

The DSC thermogram data (Table S4) were used to calculate the dimensionless molar excess Gibbs energy $\left(\frac{gE}{RT}\right)$ of the HDES and the activity coefficients of the HBAs and HBDs, as these are important thermodynamic indicators that indicate the stability and non-ideal mixing behaviour of deep eutectic solvents. A more negative $\frac{gE}{RT}$ is associated with enhanced intermolecular interactions for the solvents, and the formation of considerable melting point depressions.[68–70] Activity coefficients, however, measure the deviation from ideal mixing, with values significantly <1, indicating that the DES components interact strongly, which is essential to maintaining the solvent's eutectic state.[71]

As defined by Like *et al.*,[68] The activity coefficients and molar excess free Gibbs energy values were calculated from eqn (2) and (3), respectively.

$$\ln(\gamma_i) = -\frac{\Delta h_{fus,i}}{R}\left(\frac{1}{T} - \frac{1}{T_{m,i}}\right) - \ln(x_i) \quad (2)$$

$$\frac{gE}{RT} = \sum X_A * \ln(\Upsilon_A) + X_B * \ln(\Upsilon_B) \quad (3)$$

where: $R = 8.314$ J mol^{-1} K^{-1} (Universal gas constant); $\Delta h_{fus,i}$ = molar enthalpy (J mol^{-1}) of fusion of pure species; γ_i = activity coefficient for the component under consideration; T = eutectic melt temperature (K) derived from the DSC thermograms of the DES (Table S4); $T_{m,i}$ = melting temperature (K) of the pure component under consideration; $X_{i,e}$ = mole fraction of the solid in equilibrium with liquid mixture; $\frac{gE}{RT}$ = molar excess free Gibbs energy.

Eqn (2) and (3) assume: equilibrium between solid and liquid phases during DES melting, negligible heat-capacity difference between pure components and mixture over the transition, that the enthalpy of fusion and melting temperatures of the pure components are not altered by storage. These are standard assumptions in DES thermodynamics analysis and are justified in this work by the sharp, reproducible melting endotherms observed across all weeks and the absence of additional thermal events.[68,72,73]

The more negative the value of $\frac{gE}{RT}$; the more thermodynamically stable the solvent system is. $\frac{gE}{RT} < -1/3$ is the threshold defined by Like *et al.*[68] for a mixture considered to be DES.

*The melting temperatures and molar enthalpies data for each of the four participating components (thymol, TOAB, decanoic acid, and dodecanoic acid) were extracted from the National Institute of Standards and Technology (NIST),[74] as presented in Table 4.

For all four HDESs, the reduced excess Gibbs free energy $\frac{gE}{RT}$ as presented in Fig. 12(a) and (b), remains strongly negative and varies only modestly over the 20 weeks: from −0.997 to 1.32 for thy: C10, −1.20 to −1.39 for thy: C12, −1.97 to −2.37 for TOAB: C10, and −3.68 to −4.04 for TOAB: C12. In parallel, all activity coefficients in Fig. 12 (c) and (d) stay well below unity throughout the storage period. The combination of negative $\frac{gE}{RT}$ and activity coefficients well below unity suggest that, on average, the interactions between unlike species (HBA-HBD) are more favourable than those between like species (HBA-HBA or HBD-HBD), leading to stabilisation of the eutectic liquid relative to an ideal mixture. These values remain nearly constant with time, implying that this interaction pattern is preserved during storage.

Table 4 Molar enthalpies and melting temperatures data for thymol, TOAB, Decanoic acid, and dodecanoic acid as extracted from NIST Chemistry Webbook

	Δh_{fus} (J mol^{-1})	T_m (°K)
Thymol	22 010	323.15
TOAB	45 000	371.15
Decanoic acid	28 300	304.65
Dodecanoic acid	34 700	321.15

It is worth noting that all $\frac{gE}{RT}$ are < -0.333, indicating that the four solvent systems are classified as DES. Additionally, an activity coefficient $\gamma < 1$ indicates favourable and non-ideal interactions such as strong H-bonding or ionic interactions, which bring about stabilization to the mixed state compared to an ideal mixture. The lower activity coefficient presented in this study implies that the real mixture is more strongly interacting and more stable than an ideal solution. The small scatter in $\frac{gE}{RT}$ and γ_i is within experimental uncertainty and may reflect minor structural relaxation.

Uncertainties in $\frac{gE}{RT}$ and activity coefficients arise primarily from experimental errors in DSC transition temperatures and enthalpies, together with literature uncertainties in pure-component fusion data. Propagating the reported ±2–3 °C uncertainty in DSC transitions and the NIST fusion enthalpy tolerances leads to estimated relative errors on $\frac{gE}{RT}$ below about 10%, which is small compared to the absolute magnitude of the negative values $\left(\frac{gE}{RT} < -1/3\right)$ and does not alter the qualitative conclusion that all four HDES remain strongly non-ideal and thermodynamically stable over the storage period.

TOAB-based HDESs exhibit more negative $\frac{gE}{RT}$ values than the thymol-based systems, consistent with stronger overall non-ideal interactions in these ionic systems. The week-to-week variations in $\frac{gE}{RT}$ and γ_i are small for all four solvents, with slightly narrower ranges for the thymol HDESs, suggesting that both systems retain their eutectic characteristics during storage, with thymol systems showing marginally lower scatter. This behaviour likely reflects differences in the underlying networks: thymol HDES are dominated by robust hydrogen-bonding between the terpene and fatty-acid components,

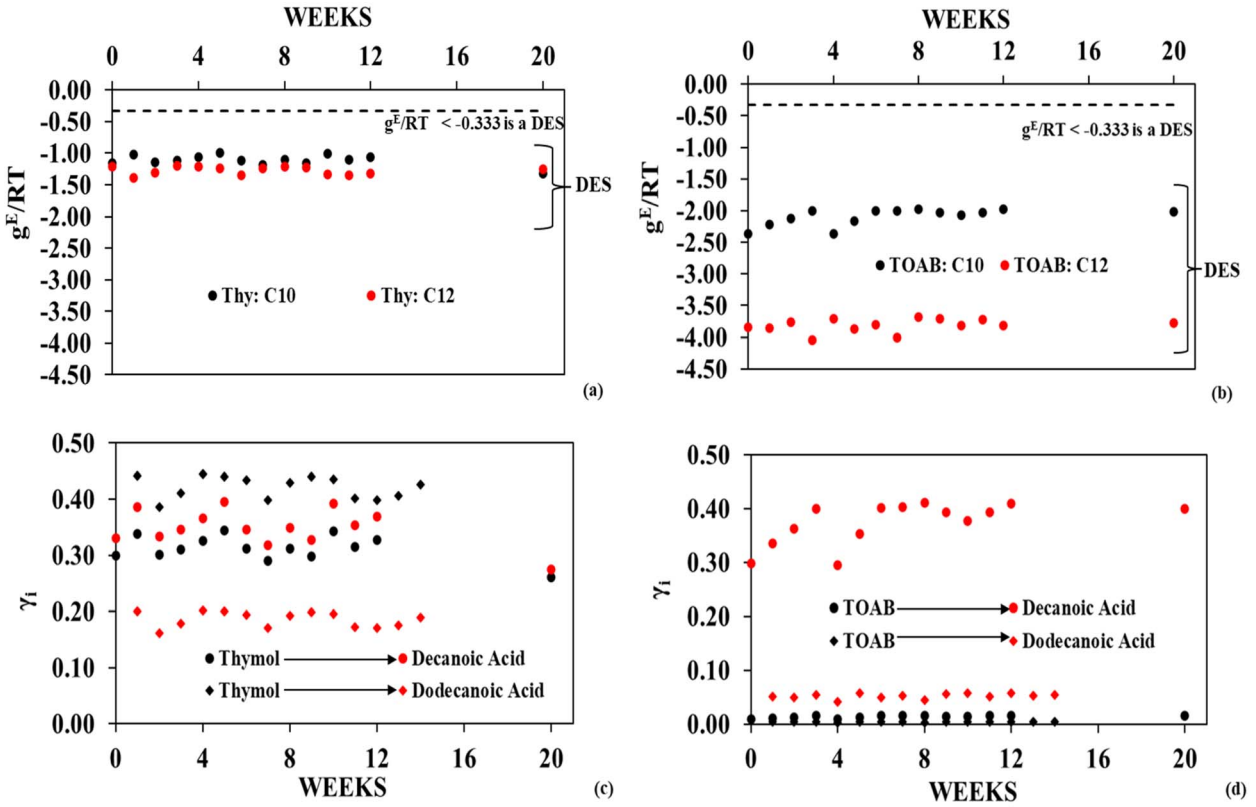

Fig. 12 Excess free Gibbs energy $\left(\frac{gE}{RT}\right)$ for (a) thy: C10 and C12 DES systems (b) TOAB: C10 and C12 DES systems; and activity coefficient for individual HDES components in liquid phase for (c) thymol, decanoic, and dodecanoic acid in both thy: C10 and C12 DES formulations and for (d) TOAB, decanoic and dodecanoic acid in both TOAB: C10 and C12 DES formulations.

whereas TOAB-based HDESs combine ion pairing and hydrogen bonding and may be more sensitive to microstructural rearrangements, although the experimental data do not indicate any systematic loss of thermodynamic stability.

4 Conclusion

This study presents a systematic time-resolved characterization of thymol- and TOAB-based hydrophobic deep eutectic solvents, demonstrating their exceptional stability over 20 weeks. The systematic multi-technique characterization, including spectroscopic, thermogravimetric, calorimetric, and bulk physicochemical property measurements, shows that these solvents maintain their molecular integrity, eutectic characteristics, and functional properties under storage conditions. More specifically, the four solvents retain stable density and viscosity within the combined experimental uncertainty, with relative standard deviations below 1% for density and modest week-to-week variations in viscosity that remain within instrument precision.

The thermodynamic stability analysed through molar excess Gibbs free energy and activity coefficients calculations demonstrates that all four HDES formulations remain firmly classified as a deep eutectic with $\frac{gE}{RT} < -1/3$ and activity coefficients below unity throughout the study period. The thermodynamic properties confirm the persistent intermolecular interactions.

Thermal stability assessment through TGA revealed that onset decomposition temperatures (T_5%) exhibit a variation of $\pm$ 2.77 °C, with TOAB-based systems showing superior thermal resistance within the range (184–205 °C) compared to the thymol-based systems (136–144 °C). These differences are attributed to the quaternary ammonium cation's capacity to form robust ionic–hydrogen bond networks with carboxylic acid HBDs, creating thermal stability with increasing fatty acid chain length.

(C12 > C 10) and enhanced thermal stability through strengthened van der Waals interaction. DSC thermograms exhibited reproducible endothermic transitions with consistent onset and peak temperatures across the storage period, confirming thermal integrity and phase behaviour stability.

From an application standpoint, the demonstrated 20-week stability is particularly relevant for HDES deployment in extraction processes (food, pharmaceutical separation, and nutraceutical), polymer processing and recycling, and biorefinery operations, where solvents are often stored in bulk and recirculated for extended periods. Typical operating temperatures in these applications (40–120 °C for liquid–liquid extraction and polymer swelling; up to about 150–200 °C for thermochemical polymer degradation) overlap with, but do not generally exceed, the TGA-derived onset temperatures T5 of the HDES (136–141 °C for thymol C10/C12 and 184–204 °C for TOAB C10/C12, Table 3). This indicates that, under carefully

controlled process conditions and residence times, the solvents can be used close to their stability limits without extensive decomposition.

FTIR spectroscopic analysis revealed consistent characteristic absorption bands and no systematic shifts, confirming the absence of hydrolysis, oxidation, or moisture-induced structural change in the studied HDESs. Apparent pH values remain within the acidic range characteristic of carboxylic acid-based HDES, with larger fluctuations in TOAB systems attributed to junction potential instability and electrode behaviour in low-conductivity media rather than true changes in proton activity. This implies that both spectroscopic and thermodynamic evidence demonstrate that the hydrogen-bonded/ionic networks defining HDESs are preserved during storage, distinguishing them from hydrophilic DES, where compositional drift and hydrolysis have been reported.

The C12-based HDESs (thy: C12 and TOAB: C12) evolve from clear liquids to semi-crystalline solids within 24 h, and become fully solid by week 20, whereas the C10 stems remain liquid. This behaviour is attributed to reversible segregation of a C12-rich solid phase driven by stronger dispersion interactions among the longer alkyl chains, which slightly shifts the effective composition of the remaining liquid but leaves DSC transitions and FT-IR spectra unchanged. While this microphase separation does not compromise chemical stability, it implies that C12 HDESs may require mild heating of storage tanks, as mentioned in Section 3.1.1 for storage and pumping in continuous processes, whereas C10 HDEs are better suited to ambient temperature.

From a sustainability and industrial implementation perspective, the demonstrated shelf-life stability of these HDES addresses a critical barrier to commercial adoption. The ability to store solvents without refrigeration or inert atmosphere requirements, coupled with their maintained physicochemical properties, translates to reduced operational costs, simplified logistics, and enhanced process reliability. The extended shelf life minimizes waste generation, conserves raw materials, and facilitates closed-loop solvent recycling strategies, all of which are core principles of green chemistry and circular economics.

Further research should focus on (1) extending monitoring beyond 20 weeks to establish ultimate shelf-life limits; (2) investigating the influence of storage conditions (temperature, light exposure, container material); (3) investigating the ageing of the solvent to predict the long-term behaviours and molecular dynamics simulations to expand the structural basis of the observed thermodynamic trends.

Lastly, this study offers the first detailed, time-resolved characterization of thymol- and TOAB-based HDESs, demonstrating their stability over 20 weeks through consistent evidence from thermodynamic, thermal, spectroscopic, and physicochemical analyses. These findings, therefore, help position HDESs as a stable alternative to traditional organic solvents, thus supporting the adoption of green chemistry principles in industrial processes.

Conflicts of interest

There are no conflicts to declare.

Data availability

All Data supporting the findings of this study are provided within the article. Underlying raw datasets that were used to generate the reported graphs and tables that are not available within the article are available from the corresponding author on reasonable request.

Supplementary information (SI): (1) FT-IR spectras for the four solvents from week 1 to 12 and week 20 (2) TGA curves for the four solvents from week 1 to 12 and week 20. (3) DSC thermograms for the four solvents from week 1 to 12 and week 20. (4) Tables of calculated (i) molar excess free Gibbs energy for the four solvents from week 1 to 12 and week 20, (ii) activity coefficients of the participating components of the four solvents. (iii) Eutectic melts temperatures derived from the DSC thermograms of all the four solvents from week 1 to 12 and week 20. See DOI: https://doi.org/10.1039/d6ra01239f.

References

1 B. B. Hansen, S. Spittle, B. Chen, D. Poe, Y. Zhang, J. M. Klein, A. Horton, L. Adhikari, T. Zelovich, B. W. Doherty, B. Gurkan, E. J. Maginn, A. Ragauskas, M. Dadmun, T. A. Zawodzinski, G. A. Baker, M. E. Tuckerman, R. F. Savinell and J. R. Sangoro, *Am. Chem. Soc.*, 2021, **121**, 1232–1285, DOI: 10.1021/acs.chemrev.0c00385.

2 C. Florindo, F. Lima, B. D. Ribeiro and I. M. Marrucho, *Curr. Opin. Green Sustainable Chem.*, 2019, **18**, 31–36, DOI: 10.1016/j.cogsc.2018.12.003.

3 A. N. Paparella, S. Perrone, A. Salomone, F. Messa, L. Cicco, V. Capriati, F. M. Perna and P. Vitale, *Catalysts*, 2023, **13**, 1035, DOI: 10.3390/catal13071035.

4 L. I. N. Tomé, V. Baião, W. da Silva and C. M. A. Brett, *Appl. Mater. Today*, 2018, **10**, 30–50, DOI: 10.1016/j.apmt.2017.11.005.

5 S. P. Ijardar, V. Singh and R. L. Gardas, *Molecules*, 2022, **27**, 1368, DOI: 10.3390/molecules27041368.

6 Y. P. Mbous, M. Hayyan, A. Hayyan, W. F. Wong, M. A. Hashim and C. Y. Looi, *Biotechnol. Adv.*, 2017, **35**, 105–134, DOI: 10.1016/j.biotechadv.2016.11.006.

7 F. M. Perna, P. Vitale and V. Capriati, *Curr. Opin. Green Sustainable Chem.*, 2020, **21**, 27–33, DOI: 10.1016/j.cogsc.2019.09.004.

8 M. Li, C. Rao, X. Ye, M. Wang, B. Yang, C. Wang, L. Guo, Y. Xiong and X. Cui, *Front. Pharmacol*, 2023, **13**, 1104096, DOI: 10.3389/fphar.2022.1104096.

9 J. Cao, J. Cao, H. Wang, L. Chen, F. Cao and E. Su, *J. Mol. Liq.*, 2020, **318**, 113997, DOI: 10.1016/j.molliq.2020.113997.

10 Z. Usmani, M. Sharma, M. Tripathi, T. Lukk, Y. Karpichev, N. Gathergood, B. N. Singh, V. K. Thakur, M. Tabatabaei and V. K. Gupta, *Sci. Total Environ.*, 2023, **881**, 163002, DOI: 10.1016/j.scitotenv.2023.163002.

11 C.-H. Nguyen, L. Augis, S. Fourmentin, G. Barratt and F.-X. Legrand, 2021, **56**, 41–102, DOI: DOI: 10.1007/978-3-030-53069-3_2.

12 A. Mišan, J. Nađpal, A. Stupar, M. Pojić, A. Mandić, R. Verpoorte and Y. H. Choi, *Crit. Rev. Food Sci. Nutr.*, 2020, **60**, 2564–2592, DOI: 10.1080/10408398.2019.1650717.
13 M. del Mar Contreras-Gámez, Á. Galán-Martín, N. Seixas, A. M. da Costa Lopes, A. Silvestre and E. Castro, *Bioresour. Technol.*, 2023, **369**, 128396, DOI: 10.1016/j.biortech.2022.128396.
14 M. Devi, R. Moral, S. Thakuria, A. Mitra and S. Paul, *Am. Chem. Soc.*, 2023, **8**, 9702–9728, DOI: 10.1021/acsomega.2c07684.
15 M. H. Zainal-Abidin, M. Hayyan and W. F. Wong, *J. Ind. Eng. Chem.*, 2021, **97**, 142–162, DOI: 10.1016/j.jiec.2021.03.011.
16 N. F. Gajardo-Parra, V. P. Cotroneo-Figueroa, P. Aravena, V. Vesovic and R. I. Canales, *J. Chem. Eng. Data*, 2020, **65**, 5581–5592, DOI: 10.1021/acs.jced.0c00715.
17 A. R. Harifi-Mood and R. Buchner, *J. Mol. Liq.*, 2017, **225**, 689–695, DOI: 10.1016/j.moliq.2016.10.115.
18 C. Ferreira and M. Sarraguça, *Pharmaceuticals*, 2024, **17**, 124, DOI: 10.3390/ph17010124.
19 N. Schaeffer, D. O. Abranches, L. P. Silva, M. A. R. Martins, P. J. Carvalho, O. Russina, A. Triolo, L. Paccou, Y. Guinet, A. Hedoux and J. A. P. Coutinho, *ACS Sustain. Chem. Eng.*, 2021, **9**, 2203–2211, DOI: 10.1021/acssuschemeng.0c07874.
20 M. Zoratti, P. A. Mercadal, C. I. Alvarez Igarzabal, M. L. Picchio and A. González, *Int. J. Biol. Macromol.*, 2024, **283**, 137970, DOI: 10.1016/j.ijbiomac.2024.137970.
21 I. D. Boateng, *J. Agric. Food Chem.*, 2022, **70**, 11860–11879, DOI: 10.1021/acs.jafc.2c05079.
22 D. J. G. P. van Osch, S. E. E. Warrag and M. C. Kroon, *ACS Sustain. Chem. Eng.*, 2020, **8**, 10591–10612, DOI: 10.1021/acssuschemeng.0c01464.
23 D. J. S. A. Audeh, A. Carniel, C. P. Borges, M. A. Z. Coelho, F. S. Buarque and B. D. Ribeiro, *Processes*, 2024, **12**, 1255, DOI: 10.3390/pr12061255.
24 L. Sportiello, F. Favati, N. Condelli, M. Di Cairano, M. C. Caruso, B. Simonato, R. Tolve and F. Galgano, *Food Chem.*, 2023, **405**, 134703, DOI: 10.1016/j.foodchem.2022.134703.
25 A. Mannu, M. Blangetti, S. Baldino and C. Prandi, *Materials*, 2021, **14**, 2494, DOI: 10.3390/ma14102494.
26 F. A. Vicente, N. Tkalec and B. Likozar, *Chem. Commun.*, 2025, **61**, 1002–1013, DOI: 10.1039/D4CC05157B.
27 H. Faraji, *TrAC, Trends Anal. Chem.*, 2024, **170**, 117429, DOI: 10.1016/j.trac.2023.117429.
28 M. Bagović Kolić, M. Železnjak, K. Markov, V. Gaurina Srček, M. Cvjetko Bubalo, K. Radošević and I. Radojčić Redovniković, *Molecules*, 2025, **30**, 1713, DOI: 10.3390/molecules30081713.
29 S. Barani Pour, J. Jahanbin Sardroodi, A. Rastkar Ebrahimzadeh, G. Pazuki and V. Hadigheh Rezvan, *Sci. Rep.*, 2024, **14**, 1763, DOI: 10.1038/s41598-023-50766-1.
30 InstaNANO, FTIR Functional Group Database Table. https://instanano.com/all/characterization/ftir/ftir-functional-group-serach/(accessed October 25th, 2025).
31 D. O. Adeoye, Z. S. Gano, O. U. Ahmed, S. M. Shuwa, A. Y. Atta and B. Y. Jubril, in *ECSOC* 2023, MDPI, Basel Switzerland, 2023, 14, p. 96, DOI: 10.3390/ecsoc-27-16380.
32 J. González-Rivera, C. Pelosi, E. Pulidori, C. Duce, M. R. Tiné, G. Ciancaleoni and L. Bernazzani, *Curr. Res. Green Sustain. Chem.*, 2022, **5**, 100333, DOI: 10.1016/J.CRGSC.2022.100333.
33 W. Chen, Z. Xue, J. Wang, J. Jiang, X. Zhao and T. Mu, Wuli Huaxue Xuebao/, *Acta Phys. Chim. Sin.*, 2018, **34**, 904–911, DOI: 10.3866/PKU.WHXB201712281.
34 A. Parr, Antonn Parr Ultrapyc 5000 series manual. https://dlu.com.ua/Ultrapyc-series (accessed January 8th, 2026).
35 A. Duque, A. Sanjuan, M. M. Bou-Ali, R. M. Alonso and M. A. Campanero, *J. Mol. Liq.*, 2023, **392**, 123431, DOI: 10.1016/j.molliq.2023.123431.
36 M. E. Di Pietro and A. Mele, *J. Mol. Liq.*, 2021, **338**, 116597, DOI: 10.1016/j.molliq.2021.116597.
37 G. Gygli, X. Xu and J. Pleiss, *Sci. Rep.*, 2020, **10**, DOI: 10.1038/s41598-020-78101-y.
38 P. Makoś-Chełstowska, E. Słupek, S. Fourmentin and J. Gębicki, *Environ. Chem. Lett.*, 2025, **23**, 41–65, DOI: 10.1007/s10311-024-01795-3.
39 M. Matsumoto, M. Ueda and Y. Tahara, *J. Chem. Eng. Jpn.*, 2023, 56, DOI: 10.1080/00219592.2023.2277827.
40 V. Hessel, N. N. Tran, M. R. Asrami, Q. D. Tran, N. Van Duc Long, M. Escribà-Gelonch, J. O. Tejada, S. Linke and K. Sundmacher, *Green Chem.*, 2022, **24**, 410–437, DOI: 10.1039/D1GC03662A.
41 E. Turiel, M. Díaz-Álvarez and A. Martín-Esteban, *Microchem. J.*, 2024, **196**, 109675, DOI: 10.1016/J.MICROC.2023.109675.
42 KINEXUS SERIES REDEFINING RHEOMETER CAPABILITIES. https://www.malvernpanalytical.com/en/ (assessed January 9th, 2026).
43 D. Shi, F. Zhou, W. Mu, C. Ling, T. Mu, G. Yu and R. Li, *Phys. Chem. Chem. Phys.*, 2022, **24**, 26029–26036, DOI: 10.1039/D2CP034423A.
44 T. Doneux, A. Sorgho, F. Soma, Q. Rayée and M. Bougouma, *Molecules*, 2024, **29**, 3439, DOI: 10.3390/molecules29143439.
45 Continued from the front IMS HORIBA Group is operating Integrated Management System (IMS) ISO9001. https://www.restek.com/techtips/Solvent-Miscibility-and20Solubility (Assessed March 21st, 2026).
46 T. Lemaoui, F. Abu Hatab, A. S. Darwish, A. Attoui, N. E. H. Hammoudi, G. Almustafa, M. Benaicha, Y. Benguerba and I. M. Alnashef, *ACS Sustain. Chem. Eng.*, 2021, **9**, 5783–5808, DOI: 10.1021/acssuschemeng.0c07367.
47 F. Bastkowski, A. Heering, E. Uysal, L. Liv, I. Leito, R. Quendera, L. Ribeiro, L. Deleebeeck, A. Snedden, D. Nagy, Z. N. Szilágyi, F. Camões, B. Anes, M. Roziková and D. Stoica, *Anal. Bioanal. Chem.*, 2024, **416**, 461–465, DOI: 10.1007/s00216-023-05043-5.
48 J. A. Illingworth, *Biochem. J.*, 1981, **195**, 259–262, DOI: 10.1042/bj/1950259.
49 S. Ruggeri, F. Poletti, C. Zanardi, L. Pigani, B. Zanfrognini, E. Corsi, N. Dossi, M. Salomäki, H. Kivelä, J. Lukkari and F. Terzi, *Electrochim. Acta*, 2019, **295**, 124–129, DOI: 10.1016/J.ELECTACTA.2018.10.086.
50 D. Turner, *J. Sci. Explor.*, 2023, **37**, 396, DOI: 10.31275/20232707.

51 G. Damilano, A. Laitinen, P. Willberg-Keyriläinen, T. Lavonen, R. Häkkinen, W. Dehaen, K. Binnemans and L. Kuutti, *RSC Adv.*, 2020, **10**, 23484–23490, DOI: 10.1039/d0ra03696j.
52 S. Inayat, S. R. Arwan, S. J. Awan, *et al.*, *Sci. Rep.*, 2023, **13**, 1777, DOI: 10.1038/s41598-023-28928-y.
53 R. Sekharan, M. Chandira, S. C. Rajesh, S. Tamilvanan, C. T. Vijayakumar and B. S. Venkateswarlu, *Biointerface Res. Appl. Chem.*, 2021, **11**, 14620–14633, DOI: 10.33263/BRIAC116.1462014633.
54 H. S. Salehi, O. A. Moultos and T. J. H. Vlugt, *J. Phys. Chem. B*, 2021, **125**, 12303–12314, DOI: 10.1021/acs.jpcb.1c07796.
55 N. C. Atilio, F. L. Fertonani and E. C. de Oliveira, *Molecules*, 2022, **27**, 8048, DOI: 10.3390/molecules27228048.
56 S. M. Patil, K. Jayachandran, M. Sahu and R. Gupta, *J. Electrochem. Soc.*, 2023, **170**, 113503, DOI: 10.1149/1945-7111/ad0adc.
57 CU Boulder, Characteristic IR Absorptions. https://www.orgchemboulder.com/Spectroscopy/Specttutor/irchart.shtml (accessed January 18th, 2026).
58 M. Yang, K. Hong, X. Li, F. Ge and Y. Tang, *RSC Adv.*, 2017, **7**, 56528–56536, DOI: 10.1039/C7RA11030H.
59 S. Shokri, N. Ebrahimi and R. Sadeghi, *J. Mol. Graph. Model.*, 2024, **131**, 108805, DOI: 10.1016/J.JMGM.2024.108805.
60 A. Shishov, P. Makoś-Chełstowska, A. Bulatov and V. Andruch, *J. Phys. Chem. B*, 2022, **126**, 3889–3896, DOI: 10.1021/1cs.jpcb.2c00858.
61 ASTM International, E2550, 2021, DOI: DOI: 10.1520/E2550-21.
62 Plastics-Thermogravimetry (TG) of polymers-Part 1: General principles, 2022 (Accessed October 28th, 2025).
63 Y. Chen, D. Yu, W. Chen, L. Fu and T. Mu, *Phys. Chem. Chem. Phys.*, 2019, **21**, 2601–2610, DOI: 10.1039/c8cp07383j.
64 A. V. Belesov, N. V. Shkaeva, M. S. Popov, T. E. Skrebets, A. V. Faleva, N. V. Ul'yanovskii and D. S. Kosyakov, *Int. J. Mol. Sci.*, 2022, **23**, 10966, DOI: 10.3390/ijms231810966.
65 M. Jablonský, A. Škulcová, A. Ház, J. Šima and V. Majová, *BioResources*, 2018, **13**, DOI: 10.15376/biores.13.4.7545-7559.
66 S. Liu, D. Yu, Y. Chen, R. Shi, F. Zhou and T. Mu, *Ind. Eng. Chem. Res.*, 2022, **61**, 14347–1435, DOI: 10.1021/acs.iecr.2c02240.
67 P. Budrugeac, *J. Therm. Anal. Calorim.*, 2009, **97**, 443–451, DOI: 10.1007/s10973-009-0081-9.
68 B. D. Like, C. E. Uhlenbrock and M. J. Panzer, *Phys. Chem. Chem. Phys.*, 2023, **25**, 7946–7950, DOI: 10.1039/D3CP00555K.
69 A. van den Bruinhorst, C. Corsini, G. Depraetère, N. Cam, A. Pádua and M. Costa Gomes, *Faraday Discuss.*, 2024, **253**, 273–288, DOI: 10.1039/D4FD00048J.
70 A. Alhadid, L. Mokrushina and M. Minceva, *Molecules*, 2019, **24**, 2334, DOI: 10.3390/molecules25051077.
71 M. Dabbagh Hosseini Pour, J. Jahanbin Sardroodi, N. Hadidi and G. Pazuki, *Sci. Rep.*, 2021, **11**, 14620–14633, DOI: 10.1038/s41598-025-25866-9.
72 A. Alhadid, L. Mokrushina and M. Minceva, *Molecules*, 2020, **25**, 1077, DOI: 10.3390/molecules25051077.
73 L. J. B. M. Kollau, M. Vis, A. Van Den Bruinhorst, G. De With and R. Tuinier, in *Pure and Applied Chemistry*, De Gruyter, 2019, vol. 91,1341–1349, DOI: 10.1515/pac-2018-1014.
74 National Institute of Standards and Technology, NIST Chemistry WebBook, https://www.webbook.nist.gov/, (accessed December 13th, 2025).